DOI:
10.1093/carcin/bgn002

Document Version
Peer reviewed version

Metabolic activation of benzo[a]pyrene *in vitro* by hepatic cytochrome P450 contrasts with detoxification *in vivo*: experiments with Hepatic Cytochrome P450 Reductase Null mice

Volker M. Arlt[*], Marie Stiborová[1], Colin J. Henderson[2], Markus Thiemann[3], Eva Frei[4], Dagmar Aimová[1], Rajinder Singh[5], Gonçalo Gamboa da Costa[†] Oliver J. Schmitz[3], Peter B. Farmer[5], C. Roland Wolf[2] and David H. Phillips

Section of Molecular Carcinogenesis, Institute of Cancer Research, Sutton, Surrey United Kingdom; [1]Department of Biochemistry, Faculty of Science, Charles University, Prague, Czech Republic; [2]Cancer Research UK Molecular Pharmacology Unit, Biomedical Research Centre, Dundee, United Kingdom; [3]Department of Analytical Chemistry, University of Wuppertal, Wuppertal, Germany; [4]Division of Molecular Toxicology, German Cancer Research Center, Heidelberg, Germany; [5]Cancer Biomarkers and Prevention Group, Biocentre, University of Leicester, Leicester LE1 7RH, United Kingdom;

* To whom correspondence should be addressed. Tel: ++44 208 722 4405; Fax: ++44 208 722 4052; Email: volker.arlt@icr.ac.uk

[†]Present Address: Division of Biochemical Toxicology, National Center for Toxicological Research, Jefferson, AR 72079.

.

Running title: Role of hepatic cytochrome P450s in benzo[*a*]pyrene detoxification *in vivo*

Key words: benzo[*a*]pyrene, cytochrome P450, cytochrome P450 oxidoreductase, DNA adducts, metabolism

Abstract

Many studies using mammalian cellular and subcellular systems have demonstrated that polycyclic aromatic hydrocarbons, including benzo[a]pyrene (BaP), are metabolically activated by cytochrome P450s (CYPs). In order to evaluate the role of hepatic *versus* extra-hepatic metabolism of BaP and its pharmacokinetics we used the HRN (Hepatic Cytochrome P450 Reductase Null) mouse model, in which cytochrome P450 oxidoreductase, the unique electron donor to CYPs, is deleted specifically in hepatocytes, resulting in the loss of essentially all hepatic CYP function. HRN and wild-type (WT) mice were treated i.p. with 125 mg/kg body weight BaP daily for up to 5 days. Clearance of BaP from blood was analysed by HPLC with fluorescence detection. DNA adduct levels were measured by ^{32}P-postlabelling analysis with structural confirmation of the formation of 10-(deoxyguanosin-N^2-yl)-7,8,9-trihydroxy-7,8,9,10-tetrahydrobenzo[*a*]pyrene (dG-N^2-BPDE) by LC-MS/MS analysis. Hepatic microsomes isolated from BaP-treated and untreated mice were also incubated with BaP and DNA *in vitro*. BaP-DNA adduct formation was up to 7-fold lower with the microsomes from HRN mice than with those from WT mice. Most of the hepatic microsomal activation of BaP *in vitro* was attributable to CYP1A. Pharmacokinetic analysis of BaP in blood revealed no significant differences between HRN and WT mice. BaP-DNA adduct levels were higher in the livers (up to 13-fold) and elevated in several extra-hepatic tissues of HRN mice (by 1.7-2.6-fold) relative to WT mice. These data reveal an apparent paradox, whereby hepatic CYP enzymes appear to be more important for detoxification of BaP *in vivo*, despite being involved in its metabolic activation *in vitro*.

Introduction

The cytochrome P450s (CYPs) superfamily consists of a large number of haem-containing mono-oxygenases that play a pivotal role in the metabolism of many drugs and carcinogens [1]. Much of the work carried out on the role of CYPs in xenobiotic metabolism has been done *in vitro*, and has yielded vital information on CYP regulation and function. However, extrapolation from *in vitro* data to *in vivo* pharmacokinetics requires additional factors such as route of administration, absorption, renal clearance and tissue-specific CYP expression to be considered [2]. A number of gene knock-out and transgenic mice have been developed to study the role of specific enzymes in xenobiotic metabolism [3,4] and, although CYP knock-out mouse models have provided important data on the effect of a single CYP enzyme on chemical-induced genotoxicity and carcinogenesis [5-10], the functional redundancy inevitably found in the CYP gene superfamily makes it difficult to determine the *in-vivo* role of these enzymes in carcinogen metabolism as a whole [11]. To overcome these limitations a mouse line, HRN (Hepatic Cytochrome P450 Reductase Null), has been developed in which cytochrome P450 oxidoreductase (POR), the unique electron donor to CYPs is deleted specifically in hepatocytes, resulting in the loss of essentially all hepatic CYP function [12]. The HRN mouse can be used to establish the role of hepatic *versus* extra-hepatic xenobiotic metabolism and disposition [11,13].

Polycyclic aromatic hydrocarbons (PAHs), of which benzo[*a*]pyrene (BaP) is the most commonly studied and measured, are formed by the incomplete combustion of organic matter [14]. They are widely distributed in the environment and human exposure to them is unavoidable. Many compounds characterised as PAHs are found in tobacco smoke condensate, although for non-smokers, the principal route of exposure is through diet [15,16]. A number of PAHs, including BaP, are mutagenic and carcinogenic, and they are widely believed to make a substantial contribution to the overall burden of cancer in humans [14,16,17]. BaP requires metabolic activation prior to reaction with DNA, which is an essential step in the mechanism by which BaP exerts its genotoxic effects [18-20]. The level of BaP-DNA adducts in cells is most likely the result of a balance between their formation and their loss through either DNA repair processes and/or apoptosis. Thus, BaP genotoxicity depends on various factors: (*i*) metabolic activation of BaP by phase I enzymes to reactive DNA binding species; (*ii*) detoxification of reactive BaP metabolites by both phase I and phase II enzymes; (*iii*) rate of repair of BaP-DNA adducts; and (*iv*) BaP-induced expression of genes such as those encoding enzymes involved in activation/detoxification or DNA damage response [10].

Based on evidence primarily from *in-vitro* experiments, CYP1A1 and CYP1B1 are two of the most important enzymes in the metabolic activation of BaP, resulting in the formation of an

epoxide that is then converted to a dihydrodiol by epoxide hydrolase [14,19]. Further bioactivation by CYP1A1 and CYP1B1 leads to the formation of the ultimately reactive species, benzo[*a*]pyrene-7,8-dihydrodiol-9,10-epoxide (BPDE) that can react with DNA, forming adducts preferentially at guanine residues, namely 10-(deoxyguanosin-N^2-yl)-7,8,9-trihydroxy-7,8,9,10-tetrahydrobenzo[*a*]pyrene (dG-N^2-BPDE) [20].

We observed recently that the carcinogen 3-nitrobenzanthrone, which is activated *in vitro* predominantly by cytosolic nitroreductases rather than microsomal POR [21], formed DNA adducts in tissues of HRN and WT mice at similar levels [21], whereas its metabolite 3-aminobenzanthrone, whose activation *in vitro* is primarily CYP-dependent [22], formed significantly lower levels of adducts in the livers of HRN than of WT mice [23]. Moreover, we found that in HRN and WT mice treated with the antineoplastic agent ellipticine, which forms DNA adducts mediated by CYPs and peroxidases, levels of hepatic ellipticine-DNA adducts were up to 65% lower in HRN mice, confirming the importance of CYPs in the bioactivation of ellipticine in the liver [24]. In the present study we report the results of experiments on BaP activation by mouse hepatic microsomes and in various mouse organs using the HRN model, from which we draw contrasting conclusions on the role of CYPs in the genotoxicity of BaP *in vivo* and *in vitro*.

Materials and methods

Chemicals

BaP (>96%) was purchased from Sigma-Aldrich (St. Louis, MO). All other chemicals were of analytical purity or better.

Animal treatment

HRN ($Por^{lox/lox}$ + Cre^{ALB}) mice on a C57BL/6 background (CXR Bioscience Ltd., Dundee, UK) used in this study were derived as described previously [12]. Mice homozygous for loxP sites at the *Por* locus ($Por^{lox/lox}$) were used as wild-type (WT). BaP was dissolved in corn-oil at a concentration of 12.5 mg/ml. Groups of female HRN and WT mice (3 months old, 25-30 g) were treated i.p. with 125 mg/kg body weight (n=3) of BaP daily either for 1 day (group I) or 5 days (group II). Control mice (n=3) received corn-oil only either for 1 day or for 5 days. Group I animals were killed 24 hours after the single dose; group II animals were sacrificed 24 hours after the last dose. Several organs (liver, forestomach, glandular stomach, lung, colon, spleen, kidney, and bladder) were removed, snap frozen and stored at −80ºC until analysis.

Measurement of BaP-DNA adducts by ^{32}P-postlabelling analysis

Genomic DNA from tissue was isolated by a standard phenol-chloroform extraction method and DNA adducts were measured for each DNA sample using the nuclease P1 enrichment version of the ^{32}P-postlabelling method as described previously with minor modifications [25]. Briefly, DNA samples (4 μg) were digested with micrococcal nuclease (120 mU, Sigma, UK) and calf spleen phosphodiesterase (40 mU, Calbiochem, UK), enriched and labelled as reported. Solvent conditions for the resolution of ^{32}P-labelled adducts on polyethyleneimine-cellulose thin-layer chromatography (TLC) were as described [25,26]. After chromatography TLC plates were scanned using a Packard Instant Imager (Dowers Grove, IL, USA) and DNA adduct levels (RAL, relative adduct labelling) were calculated from the adduct cpm, the specific activity of [γ-^{32}P]ATP and the amount of DNA (pmol of DNA-P) used. Results were expressed as DNA adducts/10^8 nucleotides. An external BPDE-DNA standard [27] was employed for identification of adducts in experimental samples. Separation of ^{32}P-labelled 3',5'-deoxyribonucleoside bisphosphate adducts by HPLC was done as described recently [28]. Briefly, individual adduct spots detected by the ^{32}P-postlabelling TLC assay were excised from the TLC plates, extracted and co-chromatographed with standard bisphosphate adduct as reported. Radioactivity eluting from the reversed-phase column was measured by monitoring Cerenkov radiation with a Flow Scintillation Analyzer (Packard, Dowers Grove, IL, USA).

Identification of BaP-DNA adducts by liquid chromatography-tandem mass spectrometry

A stable-isotope internal standard of dG[$^{15}N_5$]-N^2-BPDE was prepared as described [29]. The formation of dG-N^2-BPDE was analysed in DNA samples (50 µg) using positive electrospray ionization liquid chromatography-tandem mass spectrometry (LC-MS/MS) with selected reaction monitoring (SRM) [29]. For liver DNA samples from individual animals were analysed, whereas for the remaining tissues DNA samples were pooled from 3 animals.

Detection of BaP in blood by high-performance liquid chromatography analysis

On day 1 sequential blood samples (10 µl) were obtained by tail-bleed at 0.5, 1, 1.5, 2, 4, 6, 8, and 12 hours after injection of BaP. Blood samples were stored at −80ºC until analysis. Frozen blood samples were thawed at room temperature and 15 µl of a solution of benzo[*e*]pyrene (BeP; Dr. Ehrensdorfer GmbH, Augsburg, Germany) in acetonitrile (1 µg/ml) was added as internal standard. Whole blood was extracted three times with 100 µl ethyl acetate:acetone (2:1, v:v). Organic extracts were pooled and dried for about 2 hours in a vacuum centrifuge. The residue was resuspended in acetonitrile (150 µl) using an ultrasonic bath for 5 minutes. Each sample, alternating with the control sample, was analysed three times by high-performance liquid chromatography (HPLC; Merck Hitachi, Darmstadt, Germany) with a fluorescence detector. Injection volume was 20 µl, and samples were separated on a LiChroCART reversed-phase column (Merck LiChroCART 250-4, RP-18 [5 µm], Darmstadt, Germany). The mobile phase was acetonitrile:water (85:15, v:v) at a flow rate of 1 ml/minute. Fluorescence excitation and emission wavelengths were 294 and 404 nm, respectively. BaP concentrations in blood were calculated by comparing the peak area of BaP with those of BeP. The response factor of BaP compared with BeP was determined as 10.

Pharmacokinetic Analysis

Pharmacokinetic variables were calculated with WinNonLin software version 5.1 using the non-compartmental model 200 for extravascular input. AUC, area under the curve; $t_{½}$ terminal half-life; C_{max}, maximal blood concentration; T_{max}, time of C_{max}; Cl, clearance (CL). Differences in pharmacokinetic parameters between HRN and WT mice were analysed by the Mann-Whitney test and considered significant at $P<0.05$.

Preparation of microsomes

Hepatic microsomes from HRN and WT mice (group II), untreated or treated with BaP for 5 days as described above, were isolated as described previously [30]. Pooled microsomal fractions were used for further analyses.

Preparation of CYP1A1 and POR antibodies

Recombinant rat CYP1A1 protein was purified to homogeneity from membranes of *Escherichia coli* transfected with a modified *CYP1A1* cDNA [31]. Rabbit liver POR was purified as described

[32]. Leghorn chickens were immunized subcutaneously three times (with one week interval) with rat recombinant CYP1A1 and rabbit hepatic POR antigens (0.1 mg/animal) emulsified in complete Freund's adjuvant for the first injection and in incomplete adjuvant for boosters. Immunoglobulin fraction was purified from pooled egg yolks using fractionation by polyethylene glycol 6000 [31]. Mice anti-human prostaglandin H synthase (PTGS) 1 and 2 (PTGS1 and PTGS2) antibodies were obtained from Gentest Corp., Woburn, MA, USA).

Determination of CYP1A, POR and PTGS protein levels in hepatic microsomes

Immunoquantitation of hepatic microsomal CYP1A1 and CYP1A2, POR, PTGS1 and PTGS2 was done essentially as described previously using sodium dodecyl sulfate-polyacrylamide gel electrophoresis [31,33]. CYP, POR and PTGS were probed with the chicken anti-rat CYP1A1, chicken anti-rabbit POR and mouse anti-human PTGS polyclonal antibodies as reported [31,33]. The antibody against rat recombinant CYP1A1 recognizes both CYP1A1 and CYP1A2 in mice liver microsomes. Rat recombinant CYP1A1 and CYP1A2 (in Supersomes^{TM}, Gentest Corp.), rabbit POR, ovine PTGS1 and human recombinant PTGS2 (Gentest Corp.) were used as positive controls to identify protein bands in microsomal samples. The antigen-antibody complex was visualized with an alkaline phosphatase-conjugated rabbit anti-chicken IgG antibody and 5-bromo-4-chloro-3-indolylphosphate/nitrobluetetrazolium as chromogenic substrate [31,33]. The detection limit was 0.005 pmol CYP1A per lane [31,33] and 0.01 pmol for the other enzymes.

Determination of CYP1A and POR enzymatic activity in hepatic microsomes

The hepatic microsomal samples were characterized for CYP1A activity using 7-ethoxyresorufin *O*-deetylation (EROD) activity [31,33]. The activity of POR was measured as reported previously [34].

Real-time quantitative PCR

Total RNA was isolated from livers of HRN and WT mice killed after 5 days (either untreated or treated with BaP; group II). Tissue (~20 mg) was homogenized in 600 µl trizol (Invitrogen, UK). After addition of chloroform (120 µl), samples were centrifuged for 20 minutes at >10,000g (4ºC), and the supernatant was mixed with 70% ethanol (600 µl). Total RNA was extracted using the Qiagen RNeasy Mini Kit protocol (RNeasy Mini Handbook, Qiagen, UK) as described [35]. Two-step reverse transcription-PCR was used to generate cDNA for relative quantitation analysis using real-time fluorescent PCR on an ABI PRISM 7900HT Sequence Detection System (Applied Biosystems, UK) performed as previously described [35]. To detect the modulated expression of selected target genes 20x Assays-On-Demand^{TM} gene expression primers and probes (Applied Biosystems) were used (PTGS1-Mm00477214_m1, PTGS2-Mm00478374_m1, MPO-

Mm00447885_m1). All PCR reactions were performed in triplicate and relative gene expression was calculated using the comparative threshold cycle (C_T) method as performed previously [35].

Microsomal incubations

Incubation mixtures consisted of 50 mM potassium phosphate buffer (pH 7.4), 1 mM NADPH or NADH, pooled hepatic microsomal fraction (0.5 mg protein) from HRN and WT mice (either untreated or treated with BaP; group II), 0.1 mM BaP (dissolved in 7.5 µl DMSO) and calf thymus DNA (0.5 mg) in a final volume of 750 µl. Incubations were also carried out in the presence of a PTGS cofactor, arachidonic acid [36,37]. Mixtures then contained 0.1 mM arachidonic acid as cofactor instead of NADPH, and additionally 5 mM magnesium chloride. Incubations were carried out at 37°C for 90 min; the micosomal-mediated BaP-DNA adduct formation was linear up to 120 min. Control incubations were carried out (*i*) without microsomes; (*ii*) without NADPH or arachidonic acid; (*iii*) without DNA; and (*iv*) without BaP. After the incubation, DNA was isolated by a standard phenol-chloroform extraction method.

Inhibition studies

The following chemicals were used to inhibit the activation of BaP in mouse hepatic microsomes: α-naphthoflavone (α-NF), which inhibits CYP1A1 and CYP1A2 [22,37]; ellipticine, which competes with CYP1A1 substrates, thus inhibiting efficiently CYP1A1-mediated oxidation of other substrates [30,38]; indomethacin, a selective inhibitor of PTGS [37]; and α-lipoic acid, which inhibits POR [34]. Inhibitors were dissolved in 7.5 µl of methanol, to yield final concentrations of 0.1 mM in the incubation mixtures. Mixtures were then incubated at 37ºC for 10 min with NADPH prior to adding BaP, and then incubated for a further 90 min at 37ºC. After the incubation, DNA was isolated as mentioned above.

Results

DNA adduct formation in mice

DNA adduct formation in organs (liver, lung, forestomach, glandular stomach, kidney, bladder, spleen and colon) of HRN and WT mice treated i.p. with either a single dose or 5 daily doses of BaP was analysed by ^{32}P-postlabelling. On TLC the DNA adduct pattern consisted of a single spot with all organs from BaP-treated animals (Figure 1A and 1B, inset), whereas no DNA adducts were detected in control animals (data not shown). The identity of the material in the adduct spots was determined by HPLC to be the reactive metabolite BPDE bound to the N^2 position of guanine (dG-N^2-BPDE) both in HRN and in WT mice (Figure 1C) [27]. Independent corroboration of the structure of the DNA adducts in all 8 tissues examined was obtained by LC-MS/MS SRM [29], using a stable isotope internal standard of dG[$^{15}N_5$]-N^2-BPDE; representative results for liver only are shown in Figure 2.

DNA adduct levels were quantitated by both ^{32}P-postlabelling and by LC-MS/MS. Figure 3 shows the results of ^{32}P-postlabelling, in which it can be seen that after a single dose of BaP (Figure 3A) significantly higher levels of adducts (up to 2.6-fold) were formed in 5/7 of the extra-hepatic tissues (P<0.05) of the HRN mice that lack hepatic CYP activity. This difference was less evident after mice had received multiple doses of BaP (Figure 3B), when only 2 of the extra-hepatic tissues of HRN mice, lung and colon, had significantly more adducts than were found in WT mice. The greatest differences between HRN and WT mice, however, were found with liver DNA adducts. After a single dose of BaP, adduct levels were 13.4-fold higher in HRN mice (Figure 3A), and the difference was 6.4-fold after multiple doses (Figure 3B) (P<0.01). Quantitation of hepatic dG-N^2-BPDE levels by LC-MS/MS SRM revealed that DNA binding in HRN mice was up to 16.5-fold higher than in WT mice (see legend Figure 2). In the present study DNA adduct levels determined by LC-MS/MS SRM were generally 2–3-fold higher than those determined by TLC ^{32}P-postlabelling, an observation which is consistent with previous results [29].

BaP clearance in blood

The concentration of BaP in blood after i.p. treatment of HRN and WT mice with a single dose of BaP was determined using HPLC with fluorescence detection (Figure 4). Pharmacokinetic analysis revealed no statistically significant difference in any of the analysed parameters (e.g. clearance, terminal half-life, AUC). As can be seen in Figure 4 the C_{max} was slightly higher (around 1.25-fold) in HRN relative to WT mice, but this difference was not statistically significant.

The effect of BaP on expression of hepatic biotransforming enzymes

Using Western blot analysis with polyclonal antibodies raised against CYP1A1, POR or PTGS, the protein expression levels of these enzymes were determined in hepatic microsomes isolated from

HRN and WT mice from group II. Both CYP1A enzymes are constitutively expressed in livers of untreated HRN and WT mice, with HRN mice having marginally higher levels (1.4-fold) than WT mice (Figure 5A). Treatment with BaP led to 98-fold higher expression levels of CYP1A in livers of WT mice, but induced its levels 175-fold in HRN mice. The increase in CYP1A levels in these WT mice was associated with a strong increase in EROD activity, a measure of CYP1A enzyme activity (Figure 5C). EROD activity was also observed in HRN mice treated with BaP, but it was 3.4-fold lower than in WT mice treated with BaP, whereas no EROD activity was detectable in untreated HRN mice.

Hepatic POR expression was detected in WT mice, while as expected, its levels in HRN mice were very low, but still detectable, by immunostaining (Figure 5B). Hepatic POR levels in HRN mice were estimated to be less than 1.5% of the levels in WT mice (Figure 5B). POR activity measured with cytochrome c as a substrate was, however, not detectable in hepatic microsomes of HRN mice (Figure 5D). Surprisingly, the expression level of POR was also slightly induced in hepatic microsomes from mice treated with BaP (Figure 5B), where we found a 1.6- and 2.9-fold increase in WT and HRN mice, respectively. It is noteworthy that POR activity was detectable in HRN mice treated with BaP (Figure 5D). However, no protein expression of PTGS1 and PTGS2 was detectable in hepatic microsomes under any of the experimental conditions used (data not shown).

Besides the evaluation of the effects of BaP on hepatic CYP-related enzymes, modulation of PTGS and myeloperoxidase (MPO) mRNA expression by BaP in these mice was also investigated. Total RNA was isolated from frozen livers of group II mice and the relative amounts of *PTGS1*, *PTGS2* and *MPO* mRNAs were measured by real-time PCR. No expression of *PTGS2* and *MPO* was observed and no BaP-induced change in expression of *PTGS1* mRNA was detectable under the experimental conditions used (data not shown). No differences in *PTGS1* mRNA levels were observed between WT and HRN mice (data not shown).

Activation of BaP by hepatic microsomes

We determined DNA adduct formation by BaP in *in vitro* incubations with calf thymus DNA in the presence of microsomes isolated from livers of HRN and WT mice from group II. Hepatic microsomes from both mice strains were capable of activating BaP to form DNA adducts (Figure 6). Using TLC ^{32}P-postlabelling one major DNA adduct spot was detected, corresponding to the one found in all the BaP-treated mouse tissues (compare Figure 1), and verified by cochromatography analyses on HPLC as being dG-N^2-BPDE (data not shown). Selected *in-vitro* samples were analysed by LC-MS/MS to examine the formation of dG-N^2-BPDE. Overall, the levels of this DNA adduct determined by LC-MS/MS were 2–5-fold higher than those determined by TLC ^{32}P-

postlabelling (data not shown). Hence, these findings are consistent to the results obtained for the *in-vivo* samples (see above).

As shown in Figure 6, the formation of BaP-DNA adducts was stimulated by NADPH and NADH. DNA adduct formation catalysed by hepatic microsomes from mice pretreated with BaP was generally higher (Figure 6B) than with hepatic microsomes isolated from untreated mice (Figure 6A). NADPH, a cofactor for CYP-dependent oxidation of BaP, was the most effective cofactor in both systems. DNA adduct levels were up to 7-fold higher after activation with hepatic microsomes isolated from livers of WT than those from HRN mice. After the addition of NADH, which is a cofactor of the microsomal NADH:cytochrome b_5 oxidoreductase, a second electron donor for CYP-dependent systems [39], BaP-DNA adduct formation was up to 2.7-fold higher with hepatic microsomes from WT than with microsomes from HRN mice. Inhibition experiments supported the role of CYPs in the activation of BaP by hepatic microsomes. α-Lipoic acid, a selective inhibitor of POR [34], reduced DNA adduct formation by 70-90%. To further investigate the role of hepatic CYP1A1 and CYP1A2 enzymes in BaP activation, incubations were carried out in the absence and presence of α-NF, a specific inhibitor of CYP1A1 and CYP1A2 [22,30], and ellipticine, which is utilised as an inhibitor of CYP1A1 [30,38]. Both compounds inhibited DNA binding by 70-90%, suggesting that most of the hepatic microsomal activation of BaP *in vitro* is attributable to CYP1A enzyme activity in both mouse strains. It is noteworthy that although no DNA adducts were observed in control incubations with hepatic microsomes isolated from untreated mice, DNA adduct formation was detected in control incubations with hepatic microsomes isolated from BaP-treated mice, even without the addition of BaP to these incubations (Figure 6B).

We also considered other BaP-activating enzymes such as PTGS. Arachidonic acid, a cofactor for PTGS-dependent oxidation [23,37], did not influence BaP-DNA adduct formation by microsomes from either mouse strain, with or without BaP pretreatment (Figure 6). However, indomethacin, a selective inhibitor of PTGS [37], inhibited BaP activation in incubations with hepatic microsomes isolated from BaP-treated HRN mice by 30-40% (Figure 6B), although no such inhibition of the very low levels was obtained with microsomes isolated from BaP-treated WT mice (Figure 6B).

Discussion

CYP1A1 is believed to be one of the major enzymes responsible for the metabolic activation of BaP in organisms [14,19]. CYPs comprise a large family of subfamilies and isoenzymes showing considerable redundancy and overlapping substrate specificity [1]. To examine the effect of CYPs as a whole on hepatic BaP metabolism and metabolic activation we utilized the HRN mouse [12], which carries a deletion of the *POR* gene specifically in the liver, and thus lack CYP function in hepatocytes [11]. A limited number of treatments of mice with the dose used in this study, 125 mg/kg body weight, is carcinogenic [40] and induces mutagenicity in multiple organs [41].

In the present study we showed the specific role of hepatic CYP enzymes in the activating pathways of BaP *in vitro*. BaP-DNA adduct formation was strongly dependent on the catalytic activities of POR present in the mouse hepatic microsomes assayed. This conclusion was further supported by the inhibition of BaP-DNA adduct formation with α-lipoic acid, a specific inhibitor of POR [34]. Using specific CYP inhibitors, namely α-NF and ellipticine [33,38], most of the CYP-mediated BaP activation was attributable to CYP1A activity. This is in line with recent results from our laboratory showing that in mouse hepatoma Hepa1c1c7 cells BaP-DNA adduct formation correlated with induction of CYP1A1 [26]. Utilisation of hepatic microsomes isolated from mice pretreated with BaP to activate BaP *in vitro* demonstrated that DNA adduct levels were significantly higher than those obtained with hepatic microsomes isolated from untreated mice. DNA binding by BaP catalysed by hepatic microsomes isolated from treated WT mice was much higher than that obtained with microsomes isolated from treated HRN mice. Since hepatic CYP enzyme activity had been essentially obliterated by the conditional deletion of POR in hepatocytes, the level of BaP activation to DNA adducts in microsomes isolated from HRN mice is difficult to rationalise. One possible explanation is that endoplasmic membranes from non-parenchymal cells that still contain POR are mixed with those from hepatocytes containing CYP in the process of microsome isolation. This, in combination with the finding that BaP is a strong CYP inducer maybe also in otherwise not very active non-parenchymal cells, may explain these *in vitro* findings. The increase in DNA adduct formation upon pre-treatment with BaP catalysed by microsomes from WT mice is only 28.3-fold, while 50.5-fold in HRN mice indicating that another BaP inducible activating mechanism, independent of POR is responsible for BaP activation *in vitro* in these mice. Similarly, residual *in vitro* metabolism of the anticancer drug cyclophosphamide was observed in incubations using hepatic microsomes isolated from HRN mice [13]. Moreover, a recent study showed that pulmonary CYPs play a major role in 4-(methylnitrosamino)-1-(3-pyridyl)-1-butone (NNK)-induced lung tumours and that the number of NNK-induced lung tumours were reduced in pulmonary *POR*-null mice but were increased in hepatic *POR*-null mice relative to WT control [42]. However, lung

tumours in pulmonary *POR*-null mice were positive for POR expression because *POR* deletion occurred in only a portion of the Clara cells and the alveolar type II epithelial (AECII) cells, indicating that the NNK-induced tumours were derived from POR-expressing AECII cells.

Another explanation could be the induction of metabolising enzymes other than CYPs. In hepatic microsomes isolated from BaP-treated HRN mice DNA adduct formation was observed even without the addition of BaP suggesting that BaP and/or its metabolites can bind to hepatic microsomal membranes, but it is subsequently released to react with DNA during the *in vitro* incubation. The latter effect was much more pronounced in hepatic microsomes isolated from HRN mice, suggesting the induction of metabolising enzymes in the latter microsomes. BaP is not only a good substrate for CYP1A1 and CYP1B1, but also for PTGS2 [43]. When we used arachidonic acid, a cofactor for PTGS2, in hepatic microsomes isolated from mice treated with BaP, no increase in BaP-DNA adduct formation was observed. This is consistent with no detectable PTGS proteins in hepatic microsomes of either mouse strain.

Previous studies demonstrated that for a genotoxin activated by a CYP-independent mechanism, 3-nitrobenzanthrone, DNA adduct formation in mouse tissues was the same in HRN and WT mice [21], whereas DNA binding by another genotoxin, 3-aminobenzathrone, which is metabolically activated by CYPs, was elevated in the extra-hepatic tissues, and reduced in the livers, of HRN mice [23]. If CYP1A1 in particular, or CYPs in general, are involved in the activation of BaP *in vivo*, it would be predicted that there would be elevated levels of BaP-DNA adducts in extra-hepatic tissues and reduced levels in the liver, of HRN mice, relative to WT mice. While we did indeed detect more adducts in extra-hepatic tissues, we also found that the levels in liver were vastly elevated, not reduced.

Our studies on the consequences of organ-specific loss of all CYP function bear comparison with other studies on the systemic loss of function, or abrogation of induction, of specific CYPs. Administration of a high dose of BaP i.p. to *Cyp1a1(-/-)* mice resulted in slower clearance and higher adduct levels (4-fold) in liver than in *Cyp1a1(+/-)* mice [44]. Repeated high doses were less toxic to the homozygous knock-out mice than to the heterozygotes. The results were interpreted to indicate that absence of CYP1A1 protects the intact animal from BaP-mediated liver toxicity by decreasing the formation of large amounts of toxic metabolites, while the slower metabolic clearance of BaP resulted in greater formation of BaP-DNA adducts in the livers of the *Cyp1a1(-/-)* mice [44]. Conversely, BaP was more toxic to *Cyp1a1(-/-)* mice than to *Cyp1a1(+/+)* WT mice given by oral administration [10]. The rate of clearance was still slower (4-fold) in the knock-out mice, and higher levels of DNA adducts were observed in liver, spleen and bone marrow, but not in small intestine, accompanied by qualitative differences in the DNA adduct patterns between the two

genotypes. Combined studies with *Cyp1a1(-/-)* and *Cyp1b1(-/-)* single knock-out and *Cyp1a1/1b1(-/-)* double knock-out mice administrated BaP orally essentially mirrored these findings [45]. In the present study we chose i.p. injection as administration route to achieve a high induction of hepatic BaP metabolism. However, although we found much higher DNA adduct levels in the livers of HRN than in WT mice, we found no statistically significant difference in BaP pharmacokinetics (e.g. clearance, terminal half-life, and AUC) in HRN relative to WT mice.

BaP induces CYP1A1 through binding to the aryl hydrocarbon receptor (AhR), a transcription factor that also regulates the expression of a number of other phase I and phase II xenobiotic metabolising enzyme genes. Mice that lack AhR have been found to be refractory to BaP carcinogenesis after the compound was administered topically or subcutaneously, a finding that was interpreted as demonstrating that AhR is involved in BaP carcinogenesis and in converting BaP to its active metabolite(s) [46]. However, when BaP was administered i.p. to *AhR(-/-)* mice, total BaP-DNA adduct formation was at similar levels as in WT mice, although the levels of individual postlabelling adduct spots varied [47]. In another study in which BaP was given by gavage to *AhR(-/-)* mice, liver adduct levels were significantly higher than in the WT mice [48]. The authors observed slower clearance of BaP in the knock-out mice, as was also observed by Uno and coworkers in the *Cyp1a1(-/-)* mice [10] and suggested that this may explain, at least partly, the increase in DNA adduct levels. However, our present study with HRN mice did not indicate slower clearance of BaP, thereby excluding such an explanation for the high liver DNA adducts that we detected, if it can be assumed that concentrations of BaP in blood reflect tissue concentrations. The formation of BaP-DNA adducts in incubations of hepatic microsomes from BaP-pretreated mice, without the addition of BaP, suggests some BaP accumulated in the livers of the HRN mice. While the *in vivo* studies together represent a variety of doses, durations of treatment and routes of administration, overall the impression is that the function of hepatic CYPs is to detoxify BaP, not to activate it, which is in direct contrast to the general assumption from *in vitro* studies which point to metabolic activation of BaP by this enzyme system.

The mechanism by which DNA-binding species were generated in liver from BaP in the present study is not known, but it is clear that the process did not involve generation of a different reactive species from that formed in WT mice. The DNA adduct patterns obtained by ^{32}P-postlabelling were the same for the knock-out and WT mice for liver and, indeed, for extra-hepatic tissues, and the unequivocal identification of the major adduct as being the product of the reaction of BPDE with guanine residues in DNA was confirmed by MS. Previously, a very good correlation was obtained between BaP-DNA adduct determination by ^{32}P-postlabelling and LC-MS/MS SRM [29]. If, as is suggested by our study and those of other investigators [47,48], metabolic activation

of BaP *in vivo* is mediated by CYP-independent and/or AhR-independent pathways, it is apparent from our own studies, if not from others, that the end result, i.e. the nature of the DNA adducts formed, is the same. Besides differences in CYP enzyme activities the above-mentioned PTGS2 may be of importance to explain the high BaP-DNA adduct levels found in livers of HRN mice, which lack almost all POR-mediated CYP-catalysed bioactivation. However, we did not find any differences neither in PTGS2 protein levels nor *PTGS2* gene expression. Therefore, the role of other, as-yet-unidentified, BaP-activating enzymes awaits further investigation.

It is noteworthy that microarray gene expression technology previously showed that the absence of POR in the liver, and thus hepatic CYP function, appears to result only in minor compensatory changes in the expression of genes encoding for phase I and phase II xenobiotic-metabolising enzymes in untreated animals [49]. Among them only the glutathione S-transferases (GSTs), namely *GSTM2* and *GSTM3*, showed significant induction. Diol epoxides such as BPDE are detoxified by GSTs, in particular GSTM1 [19], and the ratio between CYP1A1 and GST enzyme activities has been described as a critical determinant of the target dose of reactive DNA-binding BPDE [50]. As epidemiological studies indicate a dependence of BaP-DNA adduct levels on the *CYP1A1* and *GSTM1* genotype [50], the expression of GSTs may also need consideration to explain the increased BaP-induced DNA adduct formation in HRN mice.

Numerous studies have shown that BaP is metabolised by CYPs to phenols, quinones, epoxides and arene oxides [19]. In mouse hepatoma Hepa1c1c7 cells, which express inducible CYP1A1, 3-hydroxybenzo[*a*]pyrene was the major metabolite formed after exposure to BaP [26] and this BaP metabolite is known to inhibit mutagenesis and tumourigenesis [51]. Thus, although the metabolites of BaP were not determined in the present study, it is tempting to speculate that increased CYP-catalysed formation of 3-hydroxybenzo[*a*]pyrene in WT mice may inhibit BaP-induced DNA adduct formation to a greater extent than in HRN mice. This would be the case especially after BaP induced CYP activity, which was much higher in livers of WT than in HRN mice.

In general, i.p. administration results in the uptake of BaP by mesenteric veins and lymphatic system that go directly to the liver, bypassing the gastrointestinal tract. It was pointed out previously that important pharmacokinetic differences depend on the route of administration [10]. After oral administration BaP uptake would be via the gastrointestinal tract and then to the liver. Therefore, it would be interesting to dissect the first pass elimination further by using a gastrointestinal tract- and liver-specific conditional *POR* knock-out mouse line. Recently, a variant on the HRN mouse line ($Por^{lox/lox}/Cre^{CYP1A1}$) has been developed in which POR can be deleted conditionally in the liver and gastrointestinal tract using the rat CYP1A1 promoter to drive Cre

recombinase expression [52]. Using this line, administration of the CYP1A1 inducers tetrachlorodibenzo-*p*-dioxin or β-NF results in both hepatic and gastrointestinal deletion of POR, whereas administration of 3-methylcholanthrene results specifically in loss of hepatic POR expression. In the future we will test BaP in this new line, which potentially provides an improved model to investigate the tissue-specific balance between BaP activation and detoxification.

In summary we have demonstrated that *in vivo* hepatic CYPs are more important for BaP detoxification than activation. Our results reveal an apparent paradox as CYPs mediate the metabolic activation of BaP *in vitro*. However, our study may also point towards the presence of other, as-yet-unidentified, hepatic BaP-activating enzymes in addition to PTGS2. Various studies, including ours, clearly show that expression and induction of CYPs can be beneficial in carcinogen metabolism because they may detoxify the noxious agent. The HRN mouse provides an excellent model for the further investigation of these effects.

Acknowledgements

We thank Florence Raynaud, Cancer Research UK Centre for Cancer Therapeutics, Institute of Cancer Research, Sutton, UK, for assistance with the pharmacokinetic analysis. This work was supported by research grants from Cancer Research UK (C.R. Wolf and D.H. Phillips), Grant Agency (203/06/0329; M. Stiborová) and Ministry of Education of the Czech Republic (MSM0021620808; M. Stiborová), German Research Foundation (O.J. Schmitz), UK Medical Research Council (G0100873; P.B. Farmer), and ECNIS (Environmental Cancer Risk, Nutrition and Individual Susceptibility), a network of excellence operating within the European Union 6th Framework Program, Priority 5: "Food Quality and Safety" (Contract No. 513943; V.M. Arlt, C.J. Henderson, R. Singh, G. Gamboa da Costa, P.B. Farmer, C.R. Wolf, and D.H. Phillips). The HRN mouse is a trademark of CXR Biosciences Ltd, Dundee Technopole, James Lindsay Place, Dundee, DD1 5JJ. C.R. Wolf is a Director, cofounder, and shareholder of, and C.J. Henderson is a consultant to, CXR Biosciences.

References

1. Nebert, D.W. and Dalton, T.P. (2006) The role of cytochrome P450 enzymes in endogenous signalling pathways and environmental carcinogenesis. *Nat Rev Cancer*, **6**, 947-60.
2. Nebert, D.W. (2006) Comparison of gene expression in cell culture to that in the intact animal: relevance to drugs and environmental toxicants. Focus on "development of a transactivator in hepatoma cells that allows expression of phase I, phase II, and chemical defense genes". *Am J Physiol Cell Physiol*, **290**, C37-41.
3. Henderson, C.J. and Wolf, C.R. (2003) Transgenic analysis of human drug-metabolizing enzymes: preclinical drug development and toxicology. *Mol Interv*, **3**, 331-43.
4. Gonzalez, F.J. and Kimura, S. (2001) Understanding the role of xenobiotic-metabolism in chemical carcinogenesis using gene knockout mice. *Mutat Res*, **477**, 79-87.
5. Buters, J.T., Sakai, S., Richter, T., Pineau, T., Alexander, D.L., Savas, U., Doehmer, J., Ward, J.M., Jefcoate, C.R. and Gonzalez, F.J. (1999) Cytochrome P450 CYP1B1 determines susceptibility to 7, 12-dimethylbenz[a]anthracene-induced lymphomas. *Proc Natl Acad Sci U S A*, **96**, 1977-82.
6. Kimura, S., Kawabe, M., Ward, J.M., Morishima, H., Kadlubar, F.F., Hammons, G.J., Fernandez-Salguero, P. and Gonzalez, F.J. (1999) CYP1A2 is not the primary enzyme responsible for 4-aminobiphenyl-induced hepatocarcinogenesis in mice. *Carcinogenesis*, **20**, 1825-30.
7. Buters, J.T., Mahadevan, B., Quintanilla-Martinez, L., Gonzalez, F.J., Greim, H., Baird, W.M. and Luch, A. (2002) Cytochrome P450 1B1 determines susceptibility to dibenzo[a,l]pyrene-induced tumor formation. *Chem Res Toxicol*, **15**, 1127-35.
8. Tsuneoka, Y., Dalton, T.P., Miller, M.L., Clay, C.D., Shertzer, H.G., Talaska, G., Medvedovic, M. and Nebert, D.W. (2003) 4-aminobiphenyl-induced liver and urinary bladder DNA adduct formation in Cyp1a2(-/-) and Cyp1a2(+/+) mice. *J Natl Cancer Inst*, **95**, 1227-37.
9. Kimura, S., Kawabe, M., Yu, A., Morishima, H., Fernandez-Salguero, P., Hammons, G.J., Ward, J.M., Kadlubar, F.F. and Gonzalez, F.J. (2003) Carcinogenesis of the food mutagen PhIP in mice is independent of CYP1A2. *Carcinogenesis*, **24**, 583-7.
10. Uno, S., Dalton, T.P., Derkenne, S., Curran, C.P., Miller, M.L., Shertzer, H.G. and Nebert, D.W. (2004) Oral exposure to benzo[a]pyrene in the mouse: detoxication by inducible cytochrome P450 is more important than metabolic activation. *Mol Pharmacol*, **65**, 1225-37.
11. Henderson, C.J., Pass, G.J. and Wolf, C.R. (2006) The hepatic cytochrome P450 reductase null mouse as a tool to identify a successful candidate entity. *Toxicol Lett*, **162**, 111-7.
12. Henderson, C.J., Otto, D.M., Carrie, D., Magnuson, M.A., McLaren, A.W., Rosewell, I. and Wolf, C.R. (2003) Inactivation of the hepatic cytochrome P450 system by conditional deletion of hepatic cytochrome P450 reductase. *J Biol Chem*, **278**, 13480-6.
13. Pass, G.J., Carrie, D., Boylan, M., Lorimore, S., Wright, E., Houston, B., Henderson, C.J. and Wolf, C.R. (2005) Role of hepatic cytochrome p450s in the pharmacokinetics and toxicity of cyclophosphamide: studies with the hepatic cytochrome p450 reductase null mouse. *Cancer Res*, **65**, 4211-7.
14. Baird, W.M., Hooven, L.A. and Mahadevan, B. (2005) Carcinogenic polycyclic aromatic hydrocarbon-DNA adducts and mechanism of action. *Environ Mol Mutagen*, **45**, 106-14.
15. Phillips, D.H. (1999) Polycyclic aromatic hydrocarbons in the diet. *Mutat Res*, **443**, 139-47.
16. Phillips, D.H. (2002) Smoking-related DNA and protein adducts in human tissues. *Carcinogenesis*, **23**, 1979-2004.
17. Schoket, B. (1999) DNA damage in humans exposed to environmental and dietary polycyclic aromatic hydrocarbons. *Mutat Res*, **424**, 143-53.

18. Denissenko, M.F., Pao, A., Tang, M. and Pfeifer, G.P. (1996) Preferential formation of benzo[a]pyrene adducts at lung cancer mutational hotspots in P53. *Science*, **274**, 430-2.
19. Luch, A. and Baird, W.M. (2005) *Metabolic activation and detoxification of polycyclic aromatic hydrocarbons*. Imperial College Press, London.
20. Phillips, D.H. (2005) *Macromolecular adducts as biomarkers of human exposure to polycyclic aromatic hydrocarbons*. Imperial College Press, London.
21. Arlt, V.M., Stiborova, M., Henderson, C.J., Osborne, M.R., Bieler, C.A., Frei, E., Martinek, V., Sopko, B., Wolf, C.R., Schmeiser, H.H. and Phillips, D.H. (2005) Environmental pollutant and potent mutagen 3-nitrobenzanthrone forms DNA adducts after reduction by NAD(P)H:quinone oxidoreductase and conjugation by acetyltransferases and sulfotransferases in human hepatic cytosols. *Cancer Res*, **65**, 2644-52.
22. Arlt, V.M., Hewer, A., Sorg, B.L., Schmeiser, H.H., Phillips, D.H. and Stiborova, M. (2004) 3-aminobenzanthrone, a human metabolite of the environmental pollutant 3-nitrobenzanthrone, forms DNA adducts after metabolic activation by human and rat liver microsomes: evidence for activation by cytochrome P450 1A1 and P450 1A2. *Chem Res Toxicol*, **17**, 1092-101.
23. Arlt, V.M., Henderson, C.J., Wolf, C.R., Schmeiser, H.H., Phillips, D.H. and Stiborova, M. (2006) Bioactivation of 3-aminobenzanthrone, a human metabolite of the environmental pollutant 3-nitrobenzanthrone: evidence for DNA adduct formation mediated by cytochrome P450 enzymes and peroxidases. *Cancer Lett*, **234**, 220-31.
24. Stiborova, M., Arlt, V.M., Henderson, C.J., Wolf, C.R., Kotrbova, V., Moserova, M., Hudecek, J., Phillips, D.H. and Frei, E. (2007) Role of hepatic cytochromes P450 in bioactivation of the anticancer drug ellipticine: Studies with the hepatic NADPH:Cytochrome P450 reductase null mouse. *Toxicol Appl Pharmacol*.
25. Arlt, V.M., Glatt, H., Muckel, E., Pabel, U., Sorg, B.L., Schmeiser, H.H. and Phillips, D.H. (2002) Metabolic activation of the environmental contaminant 3-nitrobenzanthrone by human acetyltransferases and sulfotransferase. *Carcinogenesis*, **23**, 1937-45.
26. Holme, J.A., Gorria, M., Arlt, V.M., Ovrebo, S., Solhaug, A., Tekpli, X., Landvik, N.E., Huc, L., Fardel, O. and Lagadic-Gossmann, D. (2007) Different mechanisms involved in apoptosis following exposure to benzo[a]pyrene in F258 and Hepa1c1c7 cells. *Chem Biol Interact*, **167**, 41-55.
27. Phillips, D.H. and Castegnaro, M. (1999) Standardization and validation of DNA adduct postlabelling methods: report of interlaboratory trials and production of recommended protocols. *Mutagenesis*, **14**, 301-15.
28. Arlt, V.M., Schmeiser, H.H., Osborne, M.R., Kawanishi, M., Kanno, T., Yagi, T., Phillips, D.H. and Takamura-Enya, T. (2006) Identification of three major DNA adducts formed by the carcinogenic air pollutant 3-nitrobenzanthrone in rat lung at the C8 and N2 position of guanine and at the N6 position of adenine. *Int J Cancer*, **118**, 2139-46.
29. Singh, R., Gaskell, M., Le Pla, R.C., Kaur, B., Azim-Araghi, A., Roach, J., Koukouves, G., Souliotis, V.L., Kyrtopoulos, S.A. and Farmer, P.B. (2006) Detection and quantitation of benzo[a]pyrene-derived DNA adducts in mouse liver by liquid chromatography-tandem mass spectrometry: comparison with 32P-postlabeling. *Chem Res Toxicol*, **19**, 868-78.
30. Stiborova, M., Stiborova-Rupertova, M., Borek-Dohalska, L., Wiessler, M. and Frei, E. (2003) Rat microsomes activating the anticancer drug ellipticine to species covalently binding to deoxyguanosine in DNA are a suitable model mimicking ellipticine bioactivation in humans. *Chem Res Toxicol*, **16**, 38-47.
31. Stiborova, M., Martinek, V., Rydlova, H., Hodek, P. and Frei, E. (2002) Sudan I is a potential carcinogen for humans: evidence for its metabolic activation and detoxication by human recombinant cytochrome P450 1A1 and liver microsomes. *Cancer Res*, **62**, 5678-84.

32. Yasukochi, Y., Peterson, J.A. and Masters, B. (1979) NADPH-cytochrome c (P450) reductase: spectrophotometric and stopped flow kinetic studies on the formation of reduced flavoprotein intermediates. *J Biol Chem*, **254**, 7097-7104.
33. Stiborova, M., Dracinska, H., Hajkova, J., Kaderabkova, P., Frei, E., Schmeiser, H.H., Soucek, P., Phillips, D.H. and Arlt, V.M. (2006) The environmental pollutant and carcinogen 3-nitrobenzanthrone and its human metabolite 3-aminobenzanthrone are potent inducers of rat hepatic cytochromes P450 1A1 and -1A2 and NAD(P)H:quinone oxidoreductase. *Drug Metab Dispos*, **34**, 1398-405.
34. Arlt, V.M., Stiborova, M., Hewer, A., Schmeiser, H.H. and Phillips, D.H. (2003) Human enzymes involved in the metabolic activation of the environmental contaminant 3-nitrobenzanthrone: evidence for reductive activation by human NADPH:cytochrome p450 reductase. *Cancer Res*, **63**, 2752-61.
35. Hockley, S.L., Arlt, V.M., Brewer, D., Giddings, I. and Phillips, D.H. (2006) Time- and concentration-dependent changes in gene expression induced by benzo(a)pyrene in two human cell lines, MCF-7 and HepG2. *BMC Genomics*, **7**, 260.
36. Stiborova, M., Frei, E., Breuer, A., Wiessler, M. and Schmeiser, H.H. (2001) Evidence for reductive activation of carcinogenic aristolochic acids by prostaglandin H synthase -- (32)P-postlabeling analysis of DNA adduct formation. *Mutat Res*, **493**, 149-60.
37. Stiborova, M., Frei, E., Hodek, P., Wiessler, M. and Schmeiser, H.H. (2005) Human hepatic and renal microsomes, cytochromes P450 1A1/2, NADPH:cytochrome P450 reductase and prostaglandin H synthase mediate the formation of aristolochic acid-DNA adducts found in patients with urothelial cancer. *Int J Cancer*, **113**, 189-97.
38. Stiborova, M., Sejbal, J., Borek-Dohalska, L., Aimova, D., Poljakova, J., Forsterova, K., Rupertova, M., Wiesner, J., Hudecek, J., Wiessler, M. and Frei, E. (2004) The anticancer drug ellipticine forms covalent DNA adducts, mediated by human cytochromes P450, through metabolism to 13-hydroxyellipticine and ellipticine N2-oxide. *Cancer Res*, **64**, 8374-80.
39. Schenkman, J.B. and Jansson, I. (1999) Interactions between cytochrome P450 and cytochrome b5. *Drug Metab Rev*, **31**, 351-64.
40. Hakura, A., Tsutsui, Y., Sonoda, J., Kai, J., Imade, T., Shimada, M., Sugihara, Y. and Mikami, T. (1998) Comparison between in vivo mutagenicity and carcinogenicity in multiple organs by benzo[a]pyrene in the lacZ transgenic mouse (Muta Mouse). *Mutat Res*, **398**, 123-30.
41. Hakura, A., Tsutsui, Y., Sonoda, J., Mikami, T., Tsukidate, K., Sagami, F. and Kerns, W.D. (1999) Multiple organ mutation in the lacZ transgenic mouse (Muta mouse) 6 months after oral treatment (5 days) with benzo[a]pyrene. *Mutat Res*, **426**, 71-7.
42. Weng, Y., Fang, C., Turesky, R.J., Behr, M., Kaminsky, L.S. and Ding, X. (2007) Determination of the role of target tissue metabolism in lung carcinogenesis using conditional cytochrome P450 reductase-null mice. *Cancer Res*, **67**, 7825-32.
43. Marnett, L.J. (1990) Prostaglandin synthase-mediated metabolism of carcinogens and a potential role for peroxyl radicals as reactive intermediates. *Environ Health Perspect*, **88**, 5-12.
44. Uno, S., Dalton, T.P., Shertzer, H.G., Genter, M.B., Warshawsky, D., Talaska, G. and Nebert, D.W. (2001) Benzo[a]pyrene-induced toxicity: paradoxical protection in Cyp1a1(-/-) knockout mice having increased hepatic BaP-DNA adduct levels. *Biochem Biophys Res Commun*, **289**, 1049-56.
45. Uno, S., Dalton, T.P., Dragin, N., Curran, C.P., Derkenne, S., Miller, M.L., Shertzer, H.G., Gonzalez, F.J. and Nebert, D.W. (2006) Oral benzo[a]pyrene in Cyp1 knockout mouse lines: CYP1A1 important in detoxication, CYP1B1 metabolism required for immune damage independent of total-body burden and clearance rate. *Mol Pharmacol*, **69**, 1103-14.

46. Shimizu, Y., Nakatsuru, Y., Ichinose, M., Takahashi, Y., Kume, H., Mimura, J., Fujii-Kuriyama, Y. and Ishikawa, T. (2000) Benzo[a]pyrene carcinogenicity is lost in mice lacking the aryl hydrocarbon receptor. *Proc Natl Acad Sci U S A*, **97**, 779-82.
47. Kondraganti, S.R., Fernandez-Salguero, P., Gonzalez, F.J., Ramos, K.S., Jiang, W. and Moorthy, B. (2003) Polycyclic aromatic hydrocarbon-inducible DNA adducts: evidence by 32P-postlabeling and use of knockout mice for Ah receptor-independent mechanisms of metabolic activation in vivo. *Int J Cancer*, **103**, 5-11.
48. Sagredo, C., Ovrebo, S., Haugen, A., Fujii-Kuriyama, Y., Baera, R., Botnen, I.V. and Mollerup, S. (2006) Quantitative analysis of benzo[a]pyrene biotransformation and adduct formation in Ahr knockout mice. *Toxicol Lett*, **167**, 173-82.
49. Wang, X.J., Chamberlain, M., Vassieva, O., Henderson, C.J. and Wolf, C.R. (2005) Relationship between hepatic phenotype and changes in gene expression in cytochrome P450 reductase (POR) null mice. *Biochem J*, **388**, 857-67.
50. Alexandrov, K., Cascorbi, I., Rojas, M., Bouvier, G., Kriek, E. and Bartsch, H. (2002) CYP1A1 and GSTM1 genotypes affect benzo[a]pyrene DNA adducts in smokers' lung: comparison with aromatic/hydrophobic adduct formation. *Carcinogenesis*, **23**, 1969-77.
51. Huang, M.T., Wood, A.W., Chang, R.L., Yagi, H., Sayer, J.M., Jerina, D.M. and Conney, A.H. (1986) Inhibitory effect of 3-hydroxybenzo(a)pyrene on the mutagenicity and tumorigenicity of (+/-)-7 beta, 8 alpha-dihydroxy-9 alpha, 10 alpha-epoxy-7,8,9,10-tetrahydrobenzo(a)pyrene. *Cancer Res*, **46**, 558-66.
52. Finn, R.D., McLaren, A.W., Carrie, D., Henderson, C.J. and Wolf, C.R. (2007) Conditional deletion of cytochrome p450 oxidoreductase in the liver and gastrointestinal tract: a new model for studying the functions of the p450 system. *J Pharmacol Exp Ther*, **322**, 40-7.

Legends to Figures

Figure 1:

Autoradiographic profiles of BaP-derived DNA adducts obtained by ^{32}P-postlabelling. Adduct spots obtained after TLC ^{32}P-postlabelling using nuclease P1 enrichment [inset] were excised and extracted from the plates, dissolved, and injected on HPLC. DNA adduct pattern obtained in liver DNA of (**A**) HRN and (**B**) WT mice treated (i.p) with 125 mg/kg body weight BaP once daily for 5 days. These profiles are representative of adduct profiles obtained with DNA from other mouse tissues, including lung, forestomach, glandular stomach, kidney, bladder, spleen, and colon. (**C**) DNA adduct pattern obtained in salmon testis DNA modified with BPDE *in vitro* [27]. The arrow indicates the position of the 5'-^{32}P-labelled bisphosphate dG-N^2-BPDE adduct.

Figure 2:

Determination of dG-N^2-BPDE adducts by LC-MS/MS SRM in mouse liver DNA of (**A**) HRN and (**B**) WT mice treated (i.p.) with 125 mg BaP/kg body weight daily for five days (5d). These profiles are representative of adduct profiles obtained with DNA from other mouse tissues including lung, forestomach, glandular stomach, kidney, bladder, spleen, and colon. Typical LC-MS/MS SRM ion chromatograms are shown for the transition *m/z* 570 to 454 and *m/z* 575 to 459 for dG-N^2-BPDE and dG[$^{15}N_5$]-N^2-BPDE, respectively. Peaks I and II represent stereoisomers of the dG-N^2-BPDE adduct, Peak II corresponds to the stereoisomer with the 7*R*,8*S*,9*S*-trihydroxy-trans-(10*S*)-dG[$^{15}N_5$]-N_2-BPDE configuration. After 1 day (group I; means ± SD; *n*=3) the adduct levels in liver were 1916.2 ± 130.7 and 116.3 ± 36.6 dG-N^2-BPDE adducts per 10^8 nucleotides in HRN and WT mice, respectively. After 5 days (group II; means ± SD; *n*=3) adduct levels in liver were 3115.9 ± 551.3 and 264.9 ± 39.1 dG-N^2-BPDE adducts per 10^8 nucleotides in HRN and WT mice, respectively.

Figure 3:

Quantitative TLC ^{32}P-postlabelling analysis of dG-N^2-BPDE adducts in organs of HRN and WT mice treated (i.p) (**A**) once (1d) or (**B**) daily with 125 mg BaP/kg body weight for five days (5d). F=fold increase in DNA binding in HRN mice compared to WT mice. Values are given as means ± SD (*n*=3); each DNA sample was determined by two postlabelled analyses. Comparison was performed by *t*-test analysis: * $P<0.01$, $^{\#}$ $P<0.05$ different from WT. RAL, relative adduct labelling.

Figure 4:

Comparison of BaP clearance in blood between HRN and WT mice treated once with 125 mg BaP/kg body weight. Values are given as means ± SD (*n*=3). Inset: pharmacokinetic variables in HRN and WT mice calculated with non-compartmental analysis.

Figure 5:

Expression of (**A**) CYP1A and (**B**) POR and their enzymatic activity [EROD (**C**) and POR activity (**D**)] in livers of HRN and WT mice, control (untreated), or treated (i.p) with 125 mg BaP/kg body weight daily for five days. Inset in *A* and *B*: immunoblots of microsomal CYP1A and POR from each mouse group, stained with antibody against rat CYP1A1 and rabbit POR, respectively. Pooled hepatic microsomal samples were used for analyses as described in Material and Methods. Values are given as means ± SD (*n*=3). ND= not detectable.

Figure 6:

DNA adduct formation by BaP activated with microsomes isolated from livers of HRN and WT mice, control (untreated) (**A**), or treated (i.p) with 125 mg BaP/kg body weight daily for five days (**B**) as determined by TLC ^{32}P-postlabelling. F=fold increase in DNA binding in microsomes from WT mice compared to HRN mice. Values are given as means ± SD (*n*=2); each DNA sample was determined by two postlabelled analyses. RAL, relative adduct labelling. Control=microsomes and DNA only; AA=arachidonic acid; IM=indomethacin; E=ellipticine; α-NF=α-naphthoflavone; α-LA=α-lipoic acid. ND=not detected.

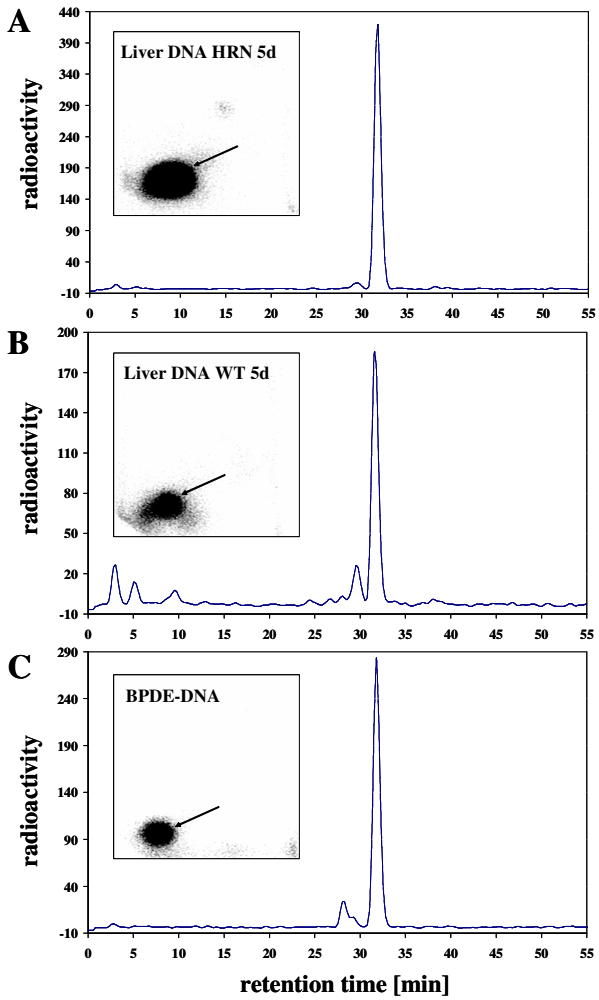
A
Liver DNA HRN 5d
radioactivity
B
Liver DNA WT 5d
radioactivity
C
BPDE-DNA
radioactivity
retention time [min]

Figure 1

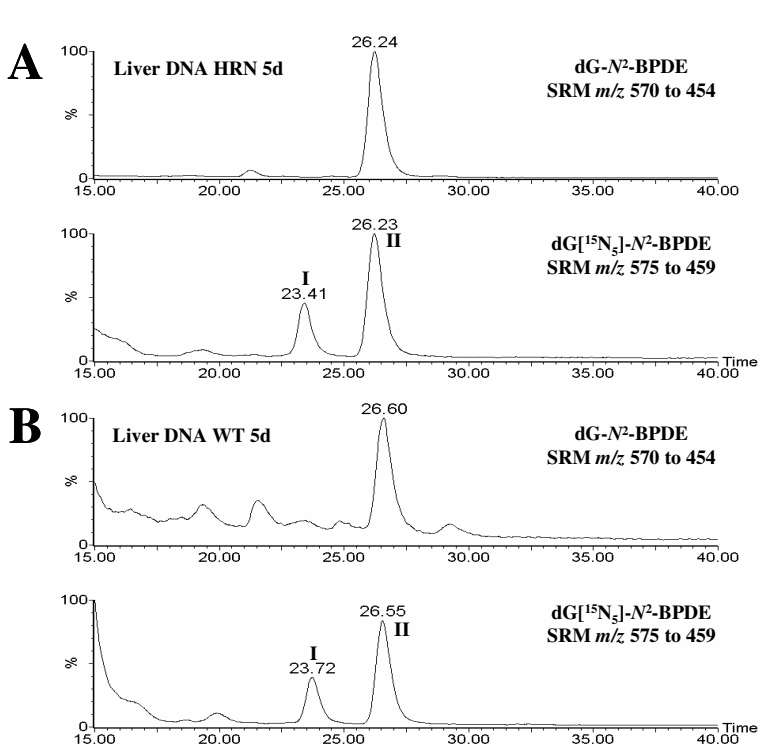
A
Liver DNA HRN 5d
26.24
dG-N2-BPDE
SRM m/z 570 to 454
26.23
II
I
23.41
dG[15N5]-N2-BPDE
SRM m/z 575 to 459
Time
B
Liver DNA WT 5d
26.60
dG-N2-BPDE
SRM m/z 570 to 454
26.55
II
I
23.72
dG[15N5]-N2-BPDE
SRM m/z 575 to 459
Time

Figure 2

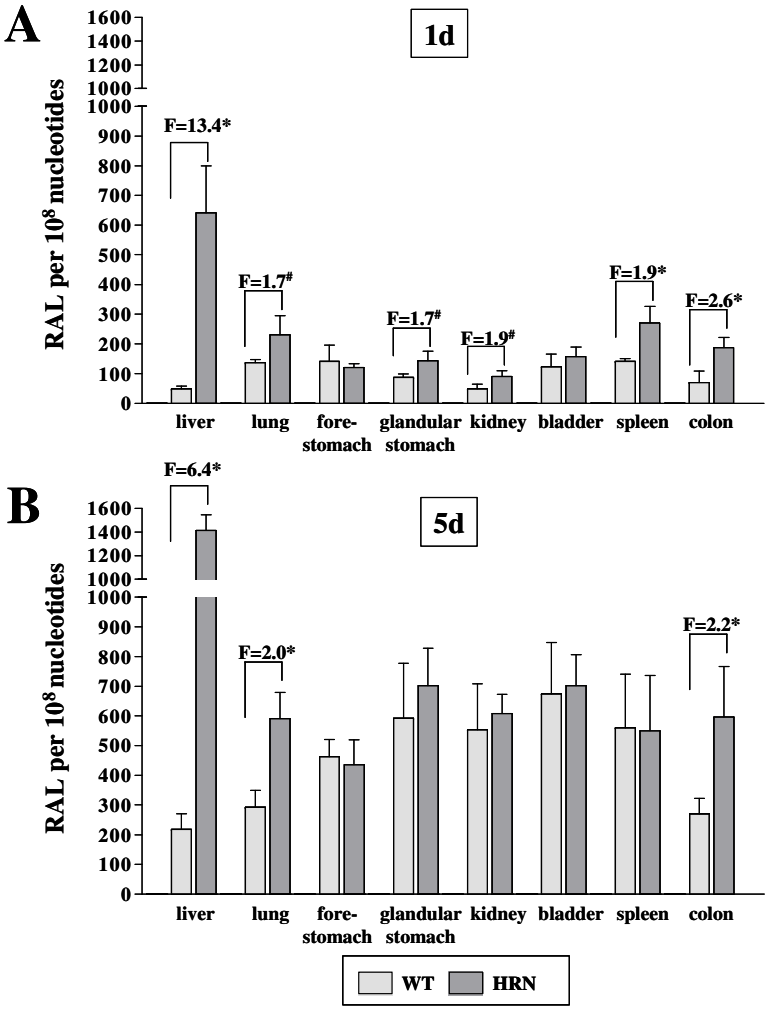
A
1d
RAL per 10^8 nucleotides
F=13.4*
F=1.7#
F=1.7#
F=1.9#
F=1.9*
F=2.6*
liver
lung
fore-stomach
glandular stomach
kidney
bladder
spleen
colon
B
5d
F=6.4*
F=2.0*
F=2.2*
WT
HRN

Figure 3

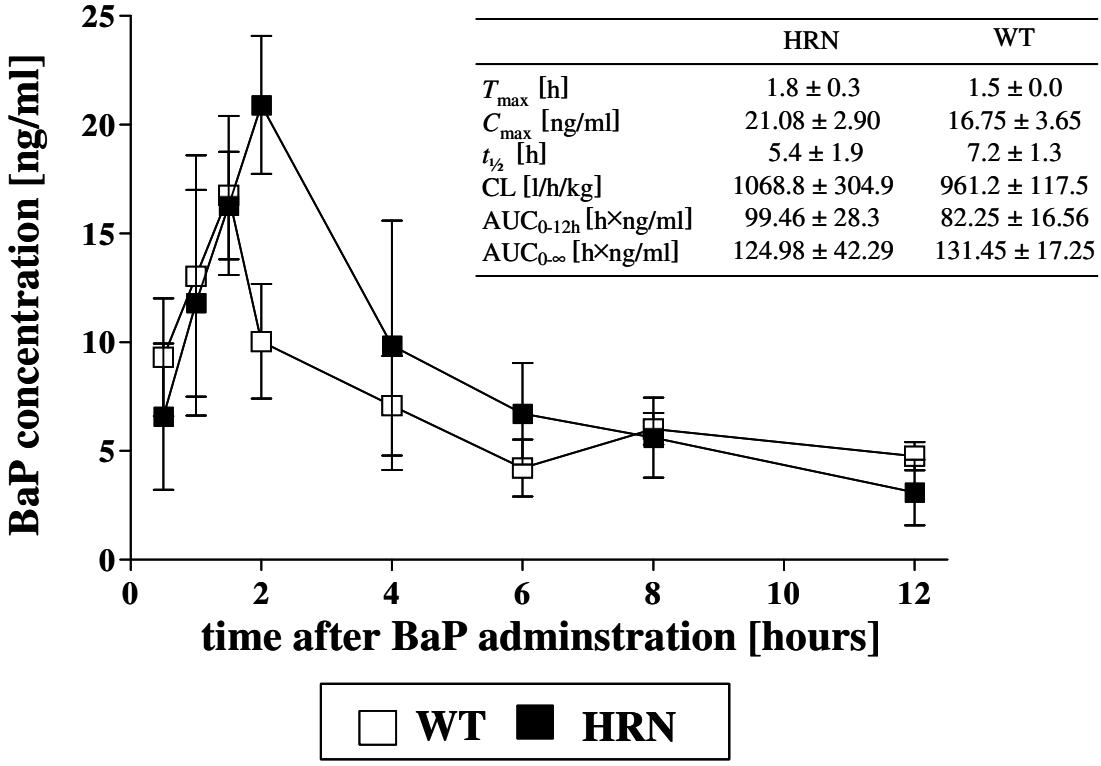

	HRN	WT
T_{max} [h]	1.8 ± 0.3	1.5 ± 0.0
C_{max} [ng/ml]	21.08 ± 2.90	16.75 ± 3.65
$t_{½}$ [h]	5.4 ± 1.9	7.2 ± 1.3
CL [l/h/kg]	1068.8 ± 304.9	961.2 ± 117.5
$AUC_{0\text{-}12h}$ [h×ng/ml]	99.46 ± 28.3	82.25 ± 16.56
$AUC_{0\text{-}\infty}$ [h×ng/ml]	124.98 ± 42.29	131.45 ± 17.25

Figure 4

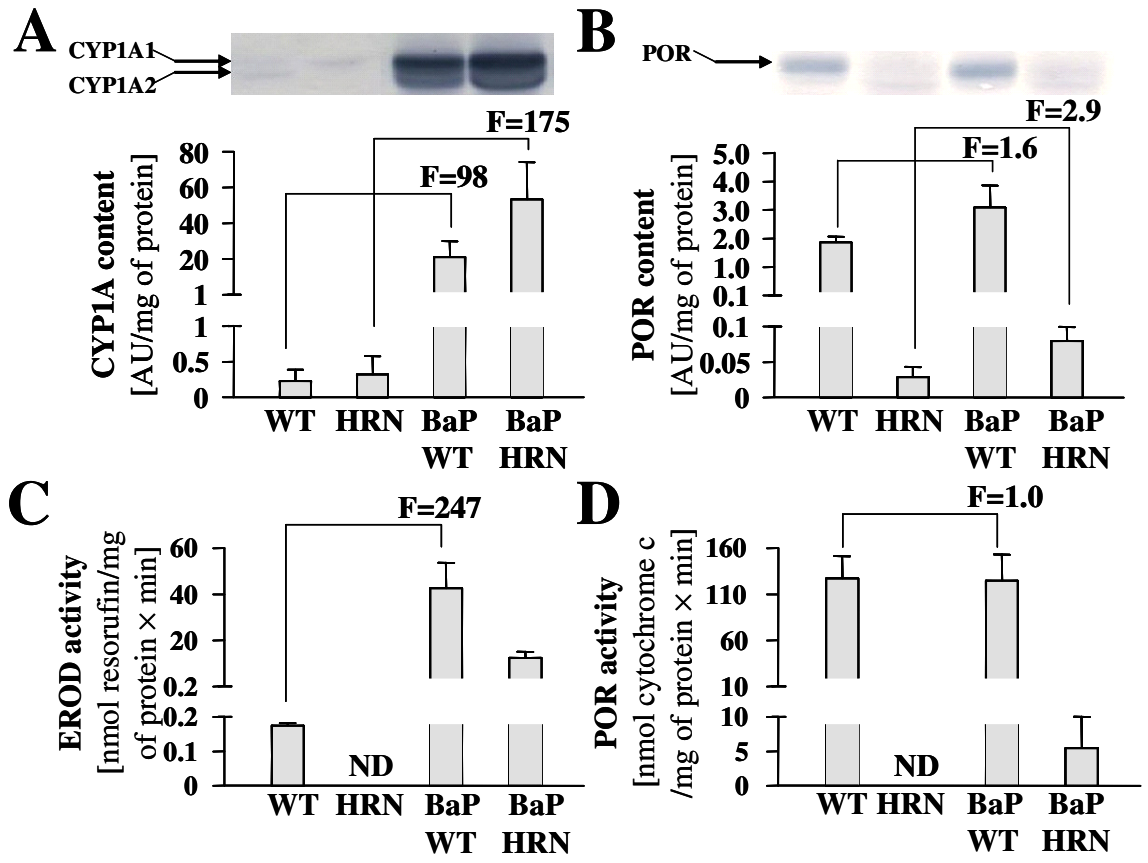
A
CYP1A1
CYP1A2
CYP1A content
[AU/mg of protein]
F=175
F=98
80
60
40
20
1
1
0.5
0
WT
HRN
BaP WT
BaP HRN
B
POR
POR content
[AU/mg of protein]
F=2.9
F=1.6
5.0
4.0
3.0
2.0
1.0
0.1
0.1
0.05
0
C
EROD activity
[nmol resorufin/mg of protein × min]
F=247
60
40
20
0.2
0.2
0.1
0
ND
D
POR activity
[nmol cytochrome c /mg of protein × min]
F=1.0
160
110
60
10
10
5
0

Figure 5

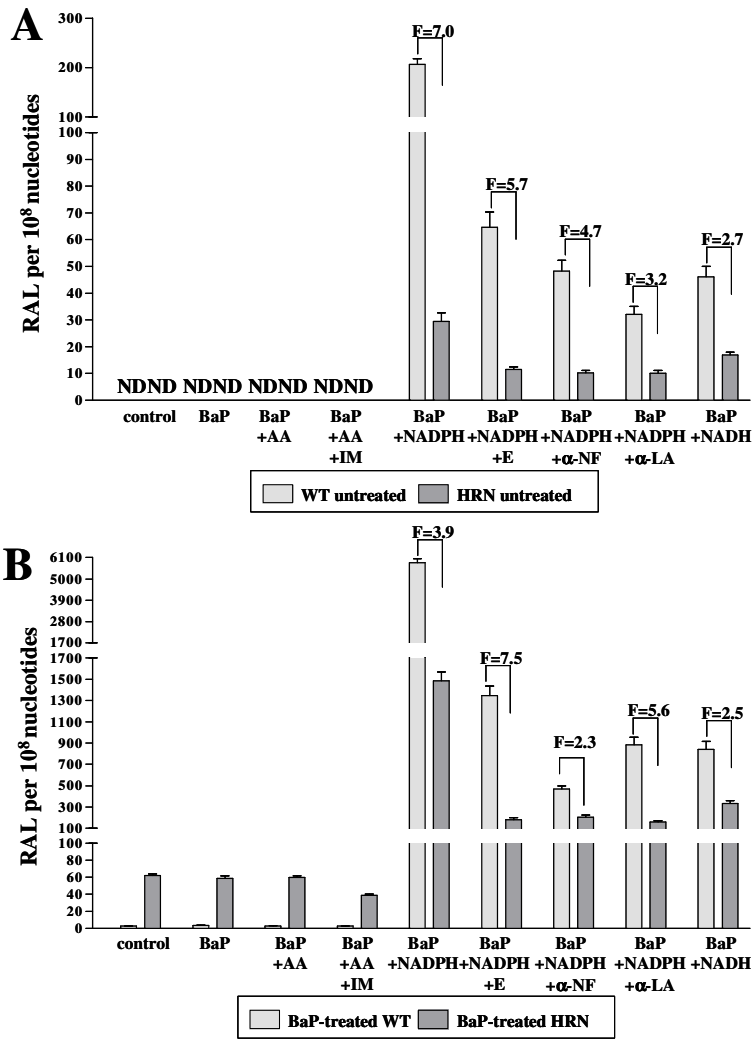
A
RAL per 10^8 nucleotides
NDND NDND NDND NDND
F=7.0
F=5.7
F=4.7
F=3.2
F=2.7
control
BaP
BaP +AA
BaP +AA +IM
BaP +NADPH
BaP +NADPH +E
BaP +NADPH +α-NF
BaP +NADPH +α-LA
BaP +NADH
WT untreated
HRN untreated
B
RAL per 10^8 nucleotides
F=3.9
F=7.5
F=2.3
F=5.6
F=2.5
BaP-treated WT
BaP-treated HRN

Figure 6